Supporting Information for

Matrix-Independent Highly Conductive Composites for Electrodes and Interconnects in Stretchable Electronics

Wei Guo[†,#], *Peng Zheng*[‡,#], *Xin Huang*[†], *Haoyue Zhuo*[‡], *Yingjie Wu*[‡], *Zhouping Yin*[†], *Zhuo Li*[*,‡] *and Hao Wu*[*,†]

[†]Flexible Electronics Research Center, School of Mechanical Science and Engineering, Huazhong University of Science and Technology, Wuhan, Hubei, 430074, P. R. China.

[‡] Department of Materials Science, Fudan University, Shanghai, 200433, China.

* E-mail: zhuo_li@fudan.edu.cn (L. Zhuo); hwu16@hust.edu.cn (H. Wu).

[#] These authors contributed equally to this work.

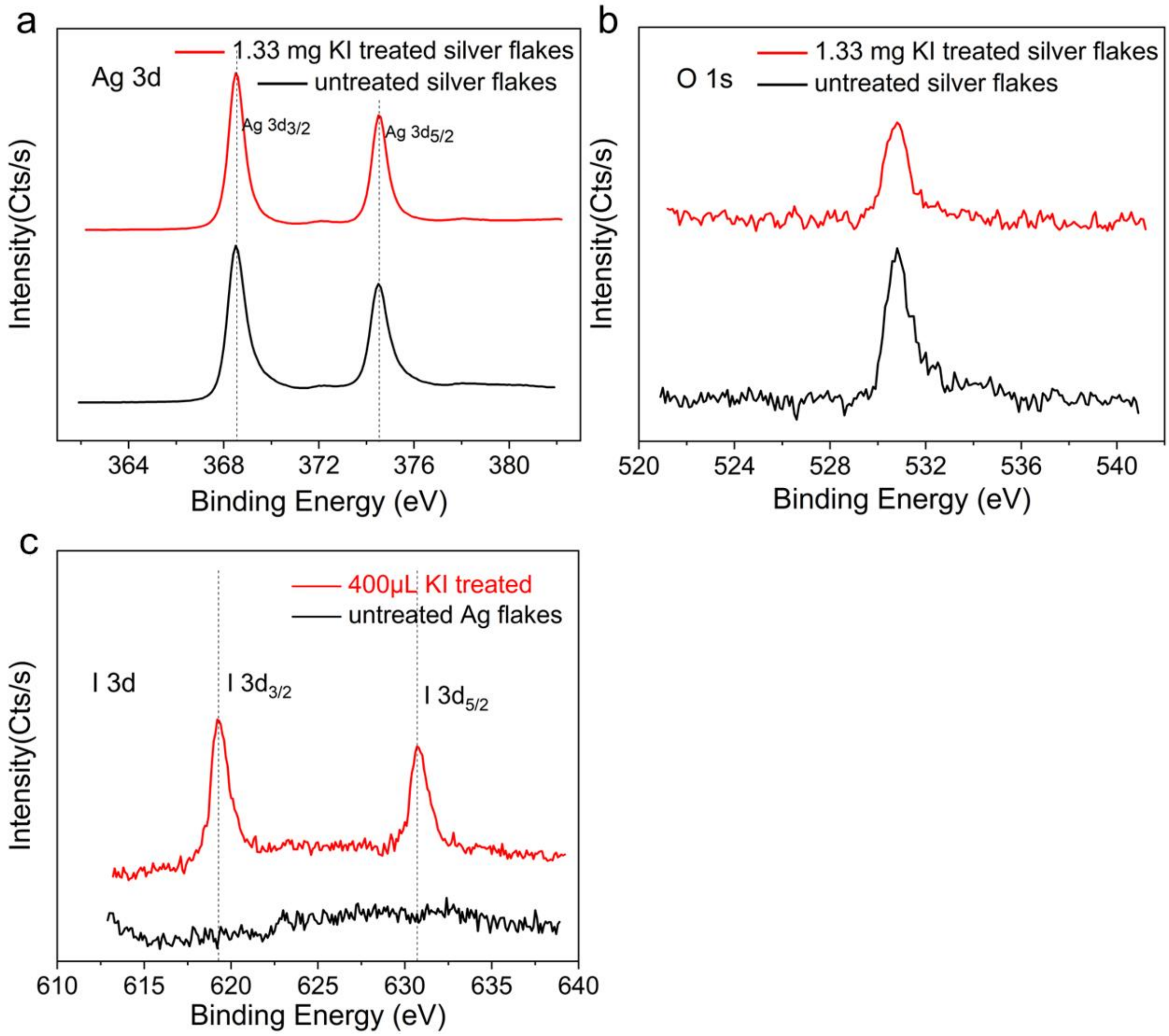

Figure S1: High resolution XPS spectra of (a) C 1s regions, (b) O 1s regions, and (c) I 3d regions of the untreated and KI-treated silver flakes (1g Ag treated with 1.33 mg KI).

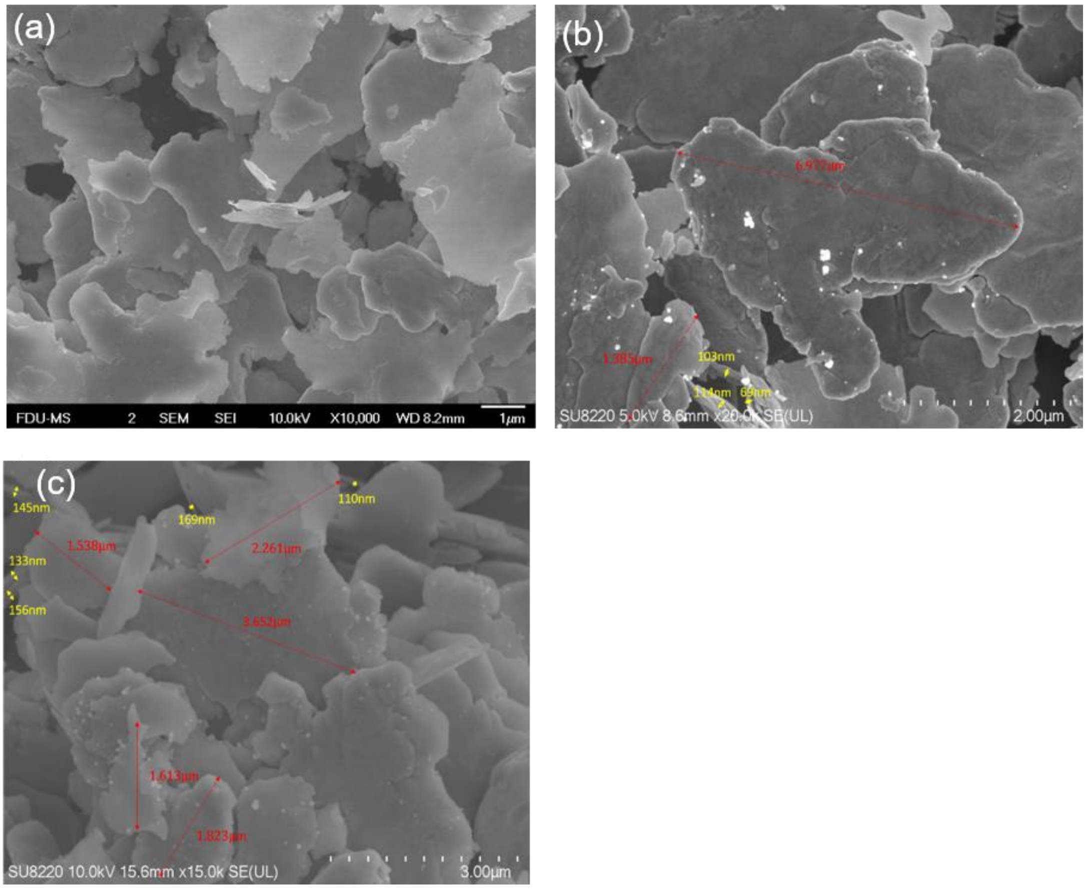

Figure S2: SEM images of (a) untreated silver flakes, (b) KI treated silver flakes with sunlight exposure, (c) KI treated silver flakes before sunlight exposure; the average diameter and thickness are 2.75 μm and 125 nm, respectively.

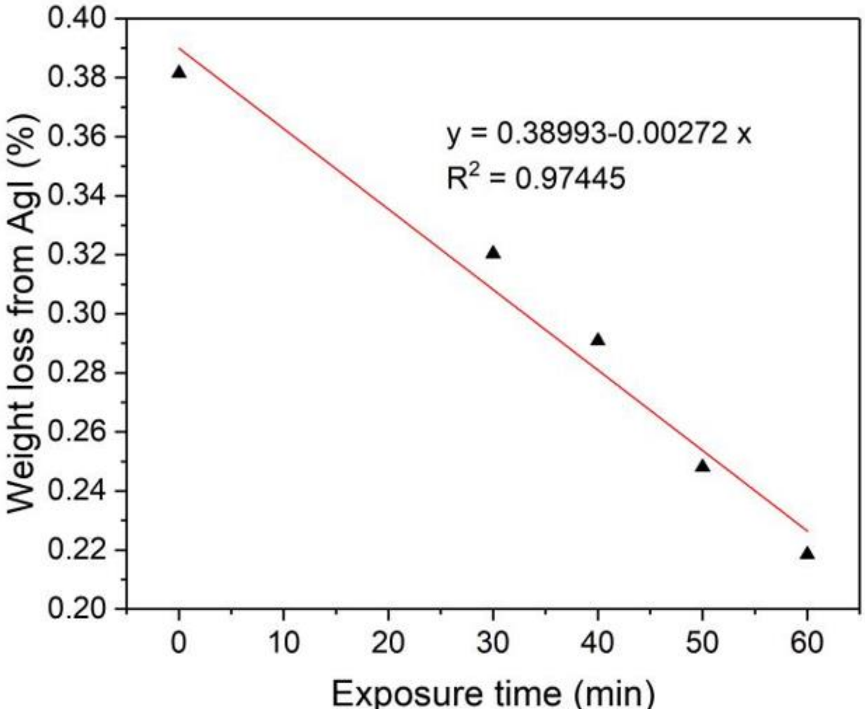

Figure S3: Weight loss at around 680 °C as a function of sunlight exposure time. As this weight loss is attributed to AgI decomposition, the decrease of weight loss with sunlight exposure time indicates that more AgI is converted to Ag when increasing the exposure time.

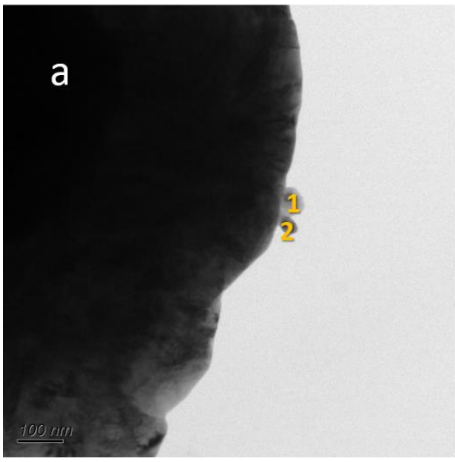

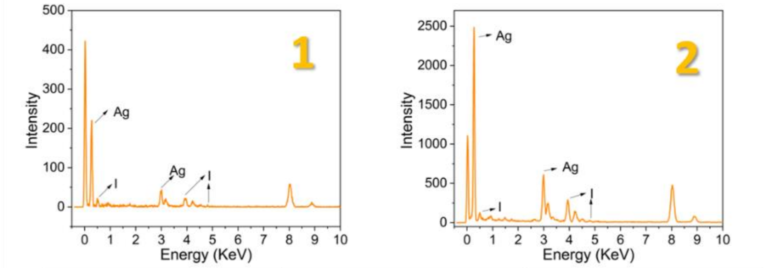

Treated Silver Flakes without sunlight exposure	Ag wt%	I wt%
1	59.39	40.61
2	60.89	39.11

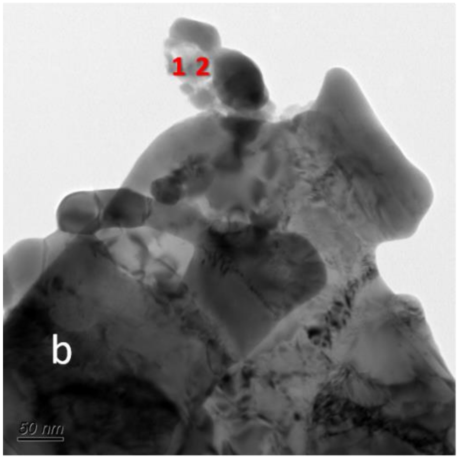

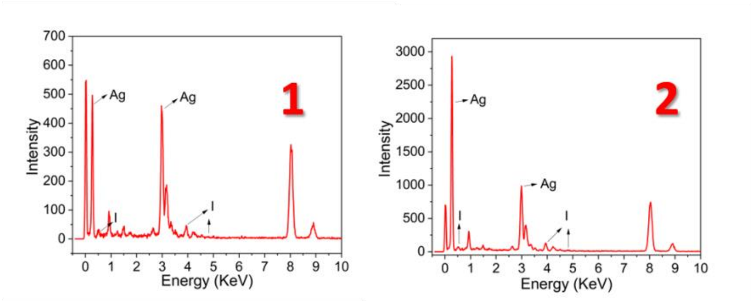

Treated Silver Flakes after sunlight exposure	Ag wt%	I wt%
1	90.18	9.82
2	85.53	14.47

Figure S4: TEM images, EDS and element weight percentage of nanoparticles on the surface of (a) treated silver flakes without sunlight exposure (orange) and (b) treated silver flakes after sunlight exposure (red).

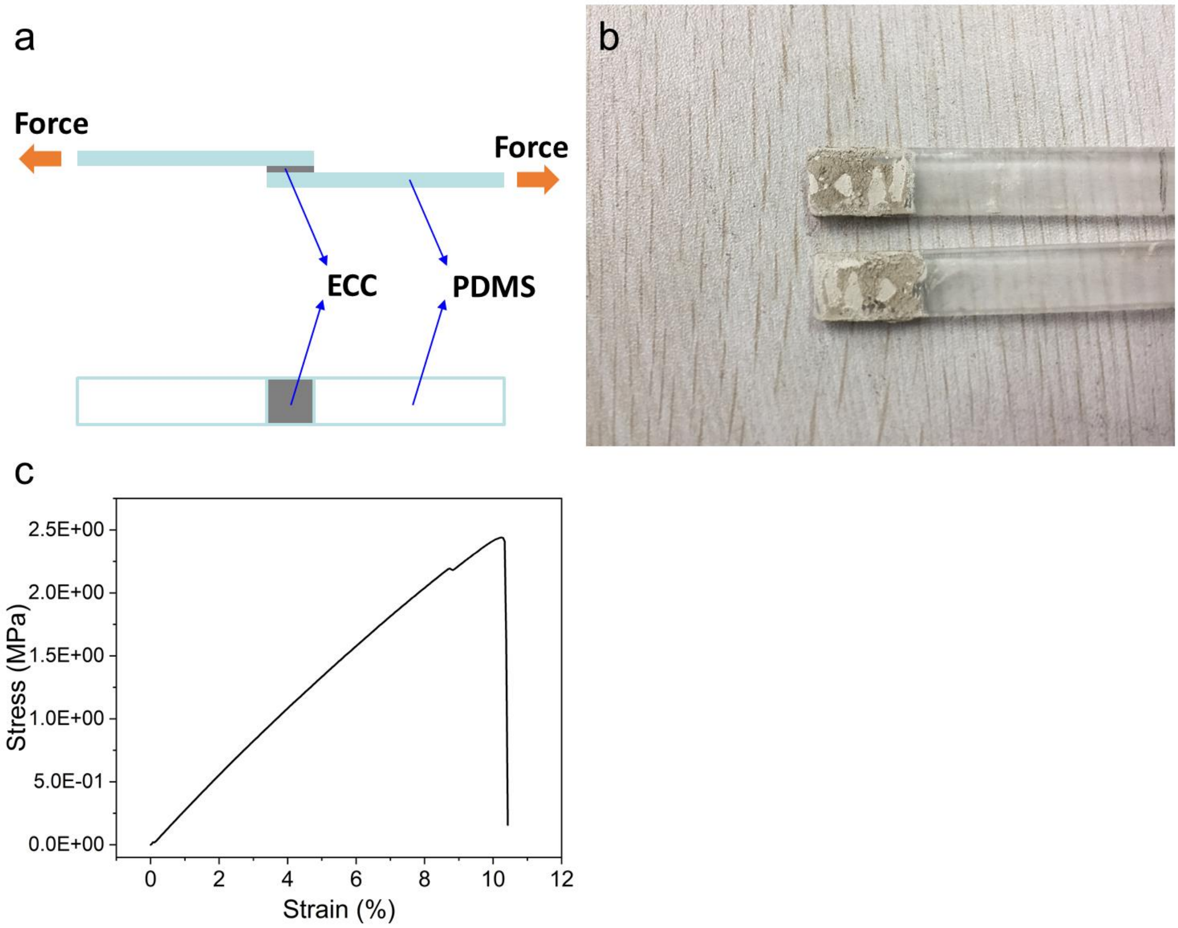

Figure S5: The lap shear test of PDMS-ECC. a) Schematic illustration of the lap shear test. b) The photography of PDMS-ECC interconnects after test showing that the PDMS-ECC and PDMS substrate interfaces are still intact even after the shear force caused PDMS-ECC to fracture. The maximum shear stress during test was 0.25 kg mm^{-2}.

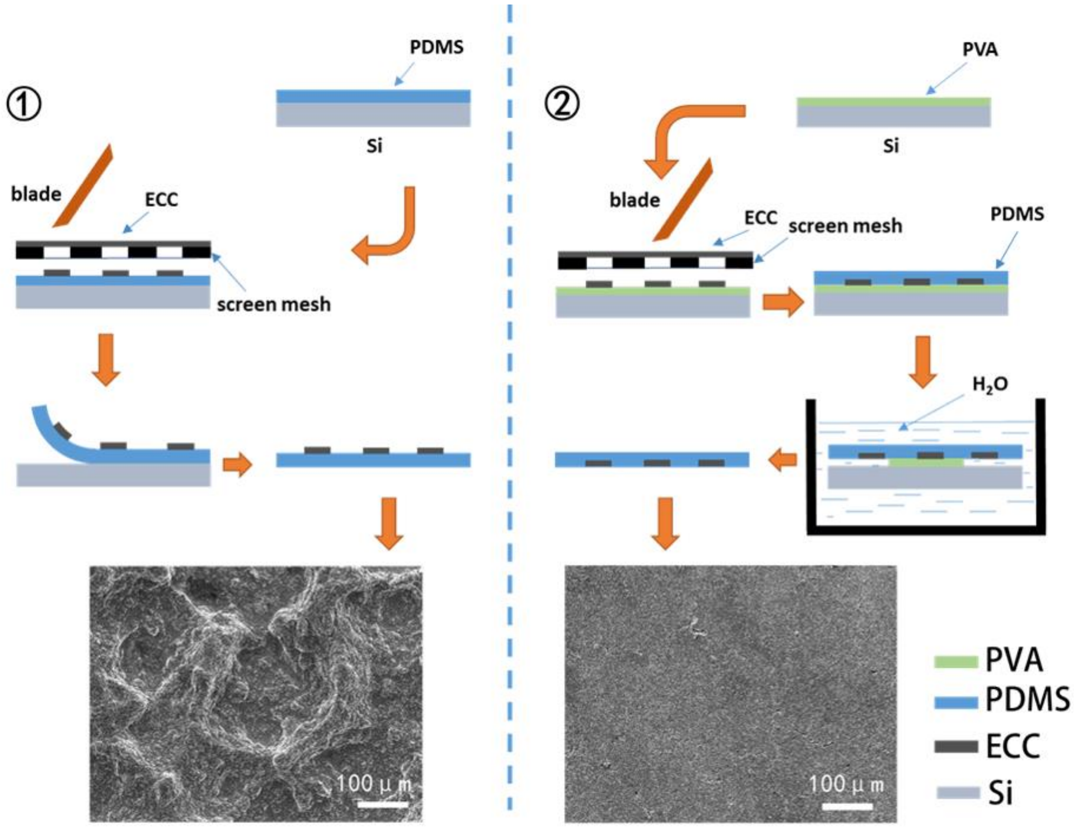

Figure S6: Two different screen printing process routes. The process route showed on right (route ②) has been adopted in this paper for the fabrication of ECCs electrodes. In routes ①, the ECCs are directly screen printed on the PDMS substrate, so the electrode surface is rougher than the other, while the second one is to print the ECCs electrodes on a polyvinyl alcohol (PVA) sacrificial layer followed by spin coating and curing of the substrate. The latter shows obvious advantages in terms of: 1) improved bonding between ECC matrix and substrate materials; 2) smooth contact surface with the skin; 3) smaller overall thickness of the ECCs electrodes, i.e., the thickness of the device is only the thickness of the spin coated substrate layer since the ECCs are embedded. It is observed that the smooth contact surface with skin leads to significantly less wear of the electrodes during EP data collection. The lower part of the figure shows the SEM images of the electrode surfaces.

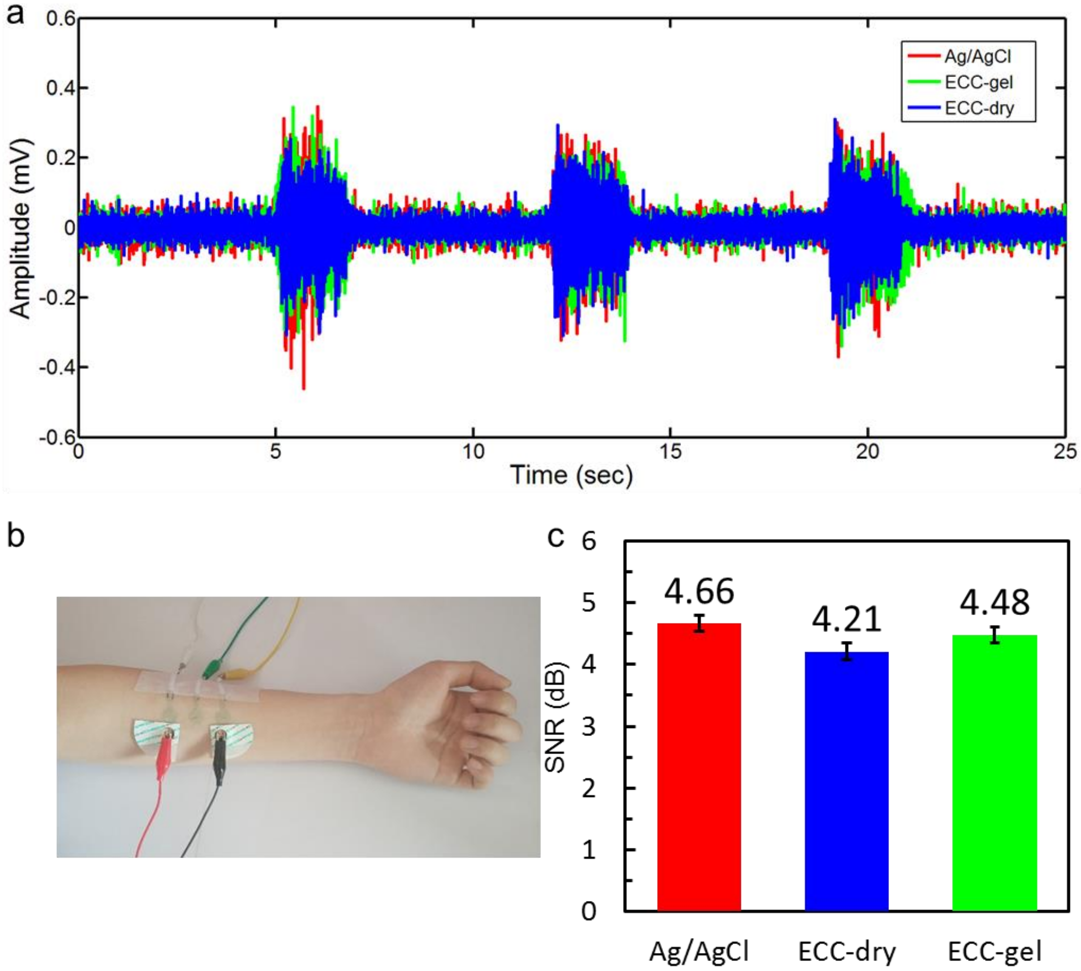

Figure S7: EMG sensing on the forearm with the ECCs electrodes (with and without gel) and commercial Ag/AgCl electrodes when the subject twists wrist three times. a) sEMG signals measured by ECCs and Ag/AgCl electrodes. b) Images showing the locations of the ECCs and Ag/AgCl electrodes. c) SNR of those three types of electrodes and test conditions.

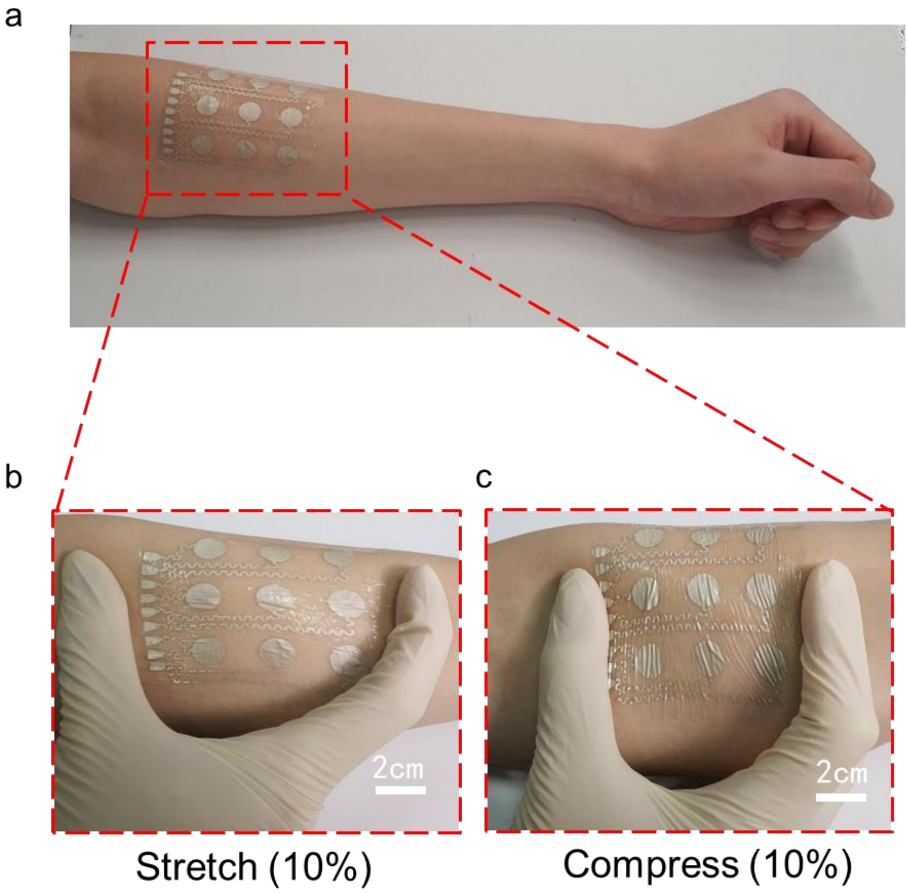

Figure S8: a) Conformal contact of the ECCs electrodes array with skin during stretch (b) and compression (c).

	Weight loss @ ~200 °C (%)	Lubricants removed after KI treatment(%)	Weight loss @ ~ 680 °C (%)	AgI (mol)	Molecular weight of lubricants	Mean molecular weight
Untreated	0.83694	0	0	0	N/A	
0.66 mg KI/g Ag	0.65323	0.18371	0.07526	0.000593	310.0075737	279.79
1.33 mg KI/g Ag	0.49675	0.34019	0.16539	0.001302	261.2257694	
1.99 mg KI/g Ag	0.33928	0.49766	0.23571	0.001856	268.138051	

Table S1: Weight loss calculation according to the TGA results shown in Figure 1c. The surface lubricant decomposition occurs at around 200 °C. The amount of lubricant removed by KI is thus estimated by the weight loss difference between KI treated silver flakes and pristine silver flakes at around 200 °C. The AgI decomposition occurs at around 680 °C. The amount of AgI generated after KI treatment is thus estimated by the weight loss difference between KI treated silver flakes and pristine silver flakes at around 680 °C. The mole number of AgI can be obtained by the generated AgI weight. If all the removed lubricant is converted to AgI, then the molecular weight of the lubricant can be calculated by dividing the lubricant weight over the mole number of AgI. The obtained molecular weight of the lubricant from all three conditions (KI concentrations) are fairly close. Moreover, the mean value is 280, close to that of the stearate ligand (283). This estimation indicates the conversion of silver lubricant (probably in the form of silver stearate) to AgI after KI treatment.

Reference	Materials	R-wave amplitude of ECG [Sensors Vs Ag/AgCl electrodes]	Contact impedance [Sensors Vs Ag/AgCl electrodes]
This Study	ECCs (without gel)	0.7mV /0.7mV (SNR: 10.57dB/11.05dB)	11.9kΩ/11.5kΩ (at 1000Hz)
ACS Nano 11 (2017): 7634.	Graphene	11mV/9mV (SNR: 15.22dB/11dB)	13kΩ/11kΩ (at 1000Hz)
	PI-Gr	(SNR: 7.2dB/11dB)	200kΩ/11kΩ (at 1000Hz)
Adv. Mater. 25 (2013): 6839.	PI-Au	-	22.4kΩ/16.9kΩ (no frequency specified)
Adv. Mater. 27 (2015): 6423.	PET-Au	0.24mV/0.32mV	-
Adv. Mater. 28 (2016): 10257.	Cu nanowire	0.4V/0.4V (compare with Cu film electrodes)	-
Adv. Funct. Mater. (2018): 1803279	Au-Parylene	1.77mV/1.79mV	44kΩ/100kΩ (at 1000Hz)
Adv. Healthcare Mater. 3 (2014): 642.	PI-Au-Silicone	1.0mV/1.7mV	-
Nat. Commun. 3 (2012): 977.	Ti-Au	0.9mV/1.1mV	-

Table S2: Comparison of measurement performance of recently reported on-skin electrophysiological electrode sensors with commercial Ag/AgCl electrodes (note: some sensors are compared with other types of electrodes).